

Many-body calculation of helium $^1D-^3D$ term intervals for $1snd$ ($n = 12 \sim 20$) high Rydberg states

Liming He and Wei Cao

Abstract: With many-body perturbation theory, $^1D-^3D$ term intervals of helium $1snd$ ($n = 12 \sim 20$) configurations are calculated. Based on two different models, Rayleigh–Schrödinger perturbation expansion terms consisting of bound states only, and those of continua are evaluated, respectively. As for bound states, zeroth-order wave functions are strictly generated from self-iteration solutions of the Hartree equation and residues of infinite expansion series are dealt with by the integral processing method, while a simplified hydrogen potential is adopted to get the continua. Using Rayleigh–Schrödinger expansions, we evaluate exchange energy up to third-order terms. It is found that level splittings are mainly attributed to summations over bound states. The fine-structure level splittings yielded here are found to agree quite well with experimental results.

PACS Nos.: 31.15.Md, 32.10Fn, 02.60Ed

Résumé : Nous calculons, dans le cadre de la théorie des perturbations à N corps, les intervalles de terme $^1D-^3D$ pour l'hélium dans les configurations $1snd$ ($n = 12 \sim 20$). Sur la base de deux modèles différents, nous évaluons les termes de l'expansion de Rayleigh–Schrödinger pour les états liés seulement et pour ceux dans le continu. Pour les états liés, les fonctions d'onde à l'ordre zéro sont obtenues à partir des solutions d'auto-interaction des équations de Hartree et les restes de l'expansion infinie sont traités par méthode intégrale, alors qu'un potentiel simplifié de type hydrogène est utilisé pour le continu. Nous avons utilisé les expansions de Rayleigh–Schrödinger pour calculer les énergies d'échange jusqu'au troisième ordre. Nous observons que la séparation des niveaux est surtout due aux sommes sur les états liés. Les séparations de structure fine trouvées ici sont en bon accord avec les résultats expérimentaux.

[Traduit par la Rédaction]

1. Introduction

Atomic Rydberg states are of great importance in both theoretical and experimental research [1–3]. As the simplest many-body system, helium is an ideal candidate for verifying quantum mechanics and theoretical methods for treating many-body problems. Research on helium level splitting structures of highly excited states has become a new focus for both theorists and experimentalists [4].

Received 24 May 2006. Accepted 21 December 2006. Published on the NRC Research Press Web site at <http://cjp.nrc.ca/> on 19 February 2007.

L. He¹ and W. Cao.² Department of Physics, East China University of Science and Technology, Shanghai 200237, P.R. China.

¹Corresponding author (e-mail: lmhe@ecust.edu.cn).

²Also at: Department of Physics, University of Fribourg, CH-1700 Fribourg, Switzerland.

Many-body perturbation theory (MBPT) [5–7] is one of the most commonly used methods to deal with many-body problems. Kelly [8] first introduced MBPT into the calculation of atomic structure. With Brueckner–Goldstone (BG) perturbation expansion, Chang and Poe [9–10] calculated fine structures of the D and F states for helium and its isoelectronic sequences, where a coarse zeroth-order wave functions were used, and it was found that the large cancellation to the first-order exchange energy due to the second-order contribution suggests that a higher order contribution should be included. To solve this problem, Chang [11] combined perturbation theory and a configuration-interaction calculation with the application of a finite basis constructed from B-splines.

The advances in variational technique made it possible to extend high-precision variational calculations into the high-energy range. The method adopted in this calculation is the combined configuration interaction (CI)–Hylleraas (Hy) basis [12, 13]. It has been shown that a careful choice of basis functions greatly improves the convergence and permits very accurate energy level calculations to be performed. According to these works, Drake gave the most elaborate and precise results [14–16]. Many of the eigenvalues have converged to better than $\pm 10^{-18}$ a.u. [15]. The singlet–triplet splittings remain clearly resolved for all states up to 10I, but are no longer visible to this degree of precision for the higher states. In contrast, the perturbation theory approach is able to yield higher accuracy. This stems from the fact that in a perturbation approach, one often reduces the calculation to the direct evaluation of the terms of interest. Thus, one may maintain the same level of high accuracy for different physical quantities, such as level splittings or shifts, whose value may differ by many orders of magnitude.

Recently, the improved density-function theory [17–19] and combination of many-body perturbation theory with the configuration-interaction (CI) method [20–22] have been adopted for studying excited states, but rarely for highly excited states. Related results of relativistic MBPT calculations from Vidolova-Angelova et al. [23] have revealed that singlet–triplet splittings increase with nuclear charge, and for sufficiently heavy atoms, these splittings may exceed the distance between adjacent Rydberg states of the same series. Koc and Migdalek [24] also utilized relativistic MBPT to evaluate the fine structure of Ag and Au atoms, but just limited it to the second-order corrections for some lower excited states.

In this paper, MBPT are used to calculate the 1D – 3D term intervals for $1snd$ ($n = 12 \sim 20$) high Rydberg states. Based on two different models, the perturbation expansion terms consisting of bound states only and those of continua are considered, respectively. According to Rayleigh–Schrödinger expansions, we have evaluated the exchange energy up to the third-order terms. It has been found that the contribution from the third-order exchange interaction is still large so cannot be neglected. The splitting levels yielded here agree quite well with experimental data.

2. Method

2.1. Perturbation expansion

We use configuration state functions (CSFs) as the basis, therefore, the atomic state function of $1snd$ states is written as [25]

$$\Psi(\gamma LS) = \sum_{i=0}^{\infty} c_i \Phi(\gamma_i LS) \quad (1)$$

where $i = 0$ is used to denote the real states, namely, $\gamma_0 = 1snd$, and we usually set $c_0 = 1$; while $\gamma_i (i \neq 0)$ for virtual states, denoted by $p_i q_i$ for two intermediate electron configurations. The perturbation approach is available if $c_i (i \neq 0) \ll 1$, which means the virtual states are the perturbation of $1snd$ configuration states.

Within the framework of perturbation theory, we get

$$H = H_0 + V \quad (2)$$

where V is the perturbation operator. According to Rayleigh–Schrödinger perturbation expansion, the perturbation corrections to the third order are as follows:

$$E^{(0)} = \varepsilon_{1s} + \varepsilon_{nd} \quad (3)$$

$$E^{(1)} = \langle \Phi_0 | V | \Phi_0 \rangle \quad (4)$$

$$E^{(2)} = \sum_{i=1}^{\infty} \frac{\langle \Phi_0 | V | \Phi_i \rangle}{E_0 - E_i} \quad (5)$$

$$E^{(3)} = \sum_{i,j=1}^{\infty} \frac{\langle \Phi_0 | V | \Phi_i \rangle \langle \Phi_i | V | \Phi_j \rangle \langle \Phi_j | V | \Phi_0 \rangle}{(E_0 - E_i)(E_0 - E_j)} - E^{(1)} \sum_{i=1}^{\infty} \frac{\langle \Phi_0 | V | \Phi_i \rangle \langle \Phi_i | V | \Phi_0 \rangle}{(E_0 - E_i)^2} \quad (6)$$

In the summations above, Φ_i and Φ_j should include all the configurations with the same parity. What is more, all the wave functions of (1) ought to have identical term values (L and S) and their components (M_L and M_S). If Φ corresponds to products of two bound states p_i and q_i (BB-type), then in (5) the symbol \sum_i should consist of the double summations over two single-particle states. If Φ involves continuum states, there should be an integral over the continua. Here, we have two possible situations, one consists of a bound state and a continuum (BC-type) and the other ought to be dual integral over two continuum orbitals (CC-type). It will be more complex for the former term of (6).

We divide the whole perturbation expansion into two parts: one with only the summations over bound states (BB-type), the other including integrations over continua (BC-type and CC-type). The calculation results reveal that the former dominates the contribution.

2.2. Solutions of the bound-state wave functions

Then we get the zeroth-order Hamiltonian

$$H_0 = h_{1s} + h_{nd} \quad (7)$$

and the perturbation term (in Rydberg units) becomes

$$V = \frac{2}{r_{12}} - V_{nd}^C - V_{1s}^C \quad (8)$$

where the Coulomb potential operators are

$$V_{nd}^C \equiv \left\langle nd \left| \frac{2}{r_{12}} \right| nd \right\rangle, \quad V_{1s}^C \equiv \left\langle 1s \left| \frac{2}{r_{12}} \right| 1s \right\rangle \quad (9)$$

standing for the potential generated from the $nd(1s)$ electron to the $1s(nd)$ electron. Hartree operators are defined as

$$h_{1s} \equiv -\nabla_{1s}^2 - \frac{4}{r_{1s}} + V_{nd}^C, \quad h_{nd} \equiv -\nabla_{nd}^2 - \frac{4}{r_{nd}} + V_{1s}^C \quad (10)$$

Orbital wave functions are obtained from the self-iteration solutions of the Hartree equation

$$\begin{cases} h_{1s}\varphi_{1s} = \varepsilon_{1s}\varphi_{1s} \\ h_{nd}\varphi_{nd} = \varepsilon_{nd}\varphi_{nd} \end{cases} \quad (11)$$

There are coupled equations in which the charge distribution of one electron depends on the other and vice versa. Hartree proposed that these equations be solved by an iterative procedure called the

self-consistent field method. Virtual states are similarly resolved for individual configurations. As h_p , h_q differ with configurations, wave functions of the same l are not orthonormal. So it is necessary to design an orthogonalization procedure to maintain the orthogonality of the total basis set. At the same time, least distortions to the states that contribute the largest perturbation to $1snd$ configurations ought to be ensured. The coupling rule of angular momenta has been applied to build up configuration state functions (CSFs), which can be expressed as products of spatial- and spin-related parts. As there are no spin-dependent interactions in the Hamiltonian, only the spatial parts are employed to evaluate the matrix elements.

It is worth mentioning that there is no corresponding 3D term in configurations of two equivalent electrons according to the Pauli exclusion principle, which yields asymmetry of the level shift of singlet and triplet by the second-order and higher order perturbation corrections. Besides, the normalization of CSFs for the equivalent electron configurations is quite different from those of the other configurations.

2.3. Solutions to the radial equation of continuum states

Continuum states cannot be orthogonalized in the same way as bound ones. It should be noted that the most dominant contribution of the continua comes from configurations such as $2p\epsilon p$, where ϵp is a continuum state whose situation is similar to an electron seeing a hydrogen potential. It is natural to adopt the hydrogen potential model, at the same time, the orthogonality of total basis states is still, conveniently, strictly maintained. As to the bound state of the BC-type, we use the simple potential [4, 10]

$$V(r) = -\frac{2Z_e}{r} \quad (12)$$

where Z_e is the effective nuclear charge, defined as

$$\begin{cases} Z_e = 2, & l = 0, 1 \\ Z_e = 1, & l = 2, 3, \dots \end{cases} \quad (13)$$

It should be mentioned that the corresponding perturbation operator under this simplified model should be changed to the one mentioned in ref. 9.

The continuum radial equation can be written as

$$\left[-\frac{d^2}{dr^2} + \frac{l(l+1)}{r^2} - \frac{2Z_e}{r} \right] P_{\epsilon r}(r) = \epsilon P_{\epsilon r} \quad (14)$$

We define $Z_e = 1$ for all continua. The normalized continuum wave functions have to fit the asymptotical formula [26]

$$P_{\epsilon l} r \xrightarrow{r \rightarrow \infty} \frac{1}{\sqrt{\pi k}} \cos(kr + \delta_0) \quad (15)$$

where $k = \sqrt{\epsilon}$. Certain numerical problems arise in the calculations of continuum functions from (15). It can be evaluated practically only for some large but finite radius $r = r_0$. To properly normalize this function, it is necessary to extrapolate to find its amplitude at infinity. This can be realized with careful consideration.

2.4. Integral processing for the residues in perturbation expansion

The perturbation expansions involve infinite series. Here, a properly approximate procedure is quite useful. Actually, as to the second-order BB-type perturbation corrections of a certain configuration series, dual summations of two infinite orbital series must be included. To facilitate this procedure, let

the summation procession of (5) be enumerated to the states where two orbitals (p and q) have the same quantum number, that is to say $n_p = n_q = n$. Then we define the summation results as $E_n^{(2)}$. A similar method can be used when we deal with the third-order corrections, although the former term of (11) consists of quadruple summations.

Define

$$\Delta E_n = E_n - E_{n-1} \quad (16)$$

Then we can get a series $\{\Delta E_n\}$, which declines with n . The summation of the whole series is the second- or third-order perturbation energy. If this series can be simulated by an analytical function, then the residue of the series can be substituted by the integral over the function, while the convergency of the series can be verified.

Choose the simulating function

$$\Delta E_n = \frac{a}{n^r} \quad (17)$$

where a and r are parameters determined by a least-squares-fitting procedure from partial terms of the series (say $n = n_0 \rightarrow n_e$). Then the integration

$$Re = \int_{n_e+1}^{\infty} \frac{a}{n^r} dn \quad (18)$$

is utilized to express the residue of summation series after n_e .

The standard error

$$\sigma = \sqrt{\frac{\sum_{n=n_0}^{n_e} (\Delta E_n - \frac{a}{n^r})^2}{n_e - n_0 + 1}} \quad (19)$$

could be denoted by the preciseness of the fitting procedure. Normally n_0 and n_e are set to be large enough and the curve extrapolation should also be investigated carefully to ensure effective simulations.

2.5. An improved Numerov algorithm

For higher Rydberg states and continua, as in the remote regions where the radial functions is still changing rapidly, the mesh points must be sufficiently close together in this region to achieve a desired accuracy. But this cannot be realized by the conventional Numerov algorithm, which leads to an inaccuracy for both the radial function and the related matrix elements [27]. Here, we use an improved Numerov algorithm [27, 28] with the merits both of insuring numerical accuracy and, as well, mastery of the requirement of numerical effort. Early methods would put equal step sizes h between points with an occasional doubling of step size. The key points of such a new algorithm is that we can set certain points, after which the step size will never be increased. This is very necessary for us to construct an effective basis set and to evaluate the perturbation matrix elements exactly by using the numerical integral method.

3. Results and discussions

Based on the theoretical methods mentioned above, the self-consistent iterative procedure has been applied to obtain the orbital wave functions for sd , pp , pf , and dd configuration series, respectively, which are then orthogonalized and used to construct corresponding CSFs. With these CSFs as a basis, perturbation energies are calculated order by order. We have mainly been concerned about the exchange term, the only contribution to the singlet-triplet level splittings. In principle, an MBPT calculation

Fig. 1. The fitting result of second-order perturbation corrections contributed by the pp configuration series as to the calculation of the $1s12d$ state. Evaluated results from 30 to 55 (\circ) have been used for fitting the simulation curve, and those from $n = 56 \sim 65$ ($*$) are applied to verify the extrapolating ability of the simulation.

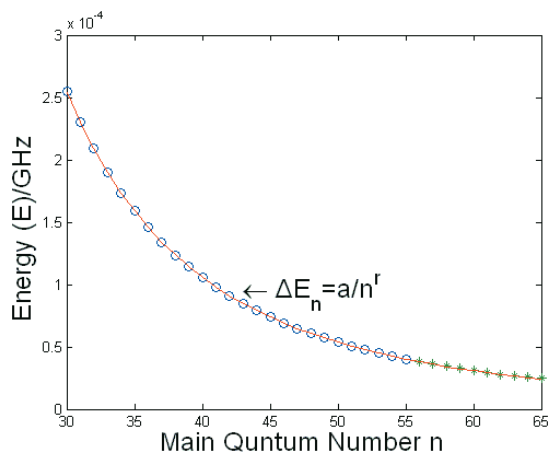


Table 1. The fitting results of pp series for the second-order MBPT calculation of $1snd$ ($n = 12 \sim 20$) configurations. r and a are the fitting parameters, and σ_f , σ_e represent standard errors for fitting and extrapolating respectively. a , σ_f , σ_e and integration Re are in units of GHz, while others are unitless.

n	r	a	σ_f	σ_e	Re
12	3.046	8.03	2.038(-7)	4.888(-7)	1.039(-3)
13	3.050	6.56	1.822(-7)	4.002(-7)	8.353(-4)
14	3.054	5.45	1.652(-7)	3.330(-7)	6.815(-4)
15	3.058	4.58	1.517(-7)	2.812(-7)	5.632(-4)
16	3.062	3.90	1.409(-7)	2.406(-7)	4.707(-4)
17	3.066	3.36	1.324(-7)	2.083(-7)	3.974(-4)
18	3.071	2.93	1.258(-7)	1.824(-7)	3.385(-4)
19	3.076	2.57	1.207(-7)	1.615(-7)	2.906(-4)
20	3.082	2.28	1.172(-7)	1.444(-7)	2.513(-4)

should involve whole summations over bound states and integral over continua. But actually, only a certain main configuration series are accessible and the residues are obtained approximately by using an integral-processing method.

Taking the calculation of the helium $1s12d$ configuration as an example, Fig. 1 presents the fitting results of second-order perturbation corrections contributed by the pp series. Setting $n_0 = 30$ and $n_e = 55$, the simulating function with its parameters (r and a) have been determined with the results evaluated from (16). We then extrapolate this curve to $n = 65$ and compare it with calculated results. The curve inosculates well with data calculated at both the fitting and extrapolating regions. So it can be concluded that the asymptotic behavior of the series (5) is well simulated by the analytical representation, and, from which, a reliable substitution of the residues (by (18)) can be obtained.

Table 1 gives the fitting results of the second-order perturbation corrections to $1snd$ ($n = 12 \sim 20$) configurations by pp series (BB-type). Parameters r and a are obtained with partial series from

Table 2. Contributions from various configurations of BB-type to the second-order exchange terms (GHz).

n	pp series	sd series	pf series	dd series	Total
12	-2.527	2.999(-3)	3.830(-4)	-3.286(-4)	-2.524
13	-1.996	2.373(-3)	2.945(-4)	-2.588(-4)	-1.994
14	-1.603	1.908(-3)	2.321(-4)	-2.074(-4)	-1.601
15	-1.307	1.557(-3)	1.866(-4)	-1.687(-4)	-1.305
16	-1.080	1.286(-3)	1.525(-4)	-1.391(-4)	-1.079
17	-0.902	1.075(-3)	1.264(-4)	-1.160(-4)	-0.901
18	-0.761	9.073(-4)	1.061(-4)	-9.776(-5)	-0.760
19	-0.648	7.726(-4)	8.994(-5)	-8.314(-5)	-0.647
20	-0.556	6.633(-4)	7.696(-5)	-7.129(-5)	-0.555

Table 3. Contributions of BC-type and CC-type configurational series to the second exchange terms(GHz).

n	pp series (BC)	pf series (BC)	sd series (BC)	dd series (BC)	pp series (CC)	Total
12	-3.402(-1)	3.129(-1)	3.881(-4)	-2.892(-4)	-3.872(-6)	-2.652(-2)
13	-2.695(-1)	2.472(-1)	3.130(-4)	-2.277(-4)	-3.061(-6)	-2.167(-2)
14	-2.170(-1)	1.986(-1)	2.556(-4)	-1.824(-4)	-2.461(-6)	-1.789(-2)
15	-1.773(-1)	1.620(-1)	2.110(-4)	-1.484(-4)	-2.007(-6)	-1.488(-2)
16	-1.466(-1)	1.338(-1)	1.760(-4)	-1.224(-4)	-1.658(-6)	-1.245(-2)
17	-1.226(-1)	1.117(-1)	1.483(-4)	-1.021(-4)	-1.385(-6)	-1.060(-2)
18	-1.035(-1)	9.429(-2)	1.260(-4)	-8.599(-5)	-1.169(-6)	-8.951(-3)
19	-8.820(-2)	8.027(-2)	1.076(-4)	-7.314(-5)	-9.959(-7)	-7.716(-3)
20	-7.575(-2)	6.892(-2)	9.379(-5)	-6.272(-5)	-8.533(-7)	-6.643(-3)

$n_0 = 30$ to $n_e = 55$. Column 4 and 5 are standard errors for the fitting areas and extrapolating regions, respectively, while the last column presents the residues of the integral processing procedure denoted above.

Contributions from various configurations of BB-type to the second-order exchange terms are given in Table 2. The residues for perturbation expansion series have been included for each configuration. The results indicate that the pp configuration series dominates the contribution, while the contributions from the dd series are five-orders smaller than those from the pp series. As only four effective floating numbers are maintained here, the effects of the dd and other series, such as ff etc., could be neglected.

As to the problems related to continua, BC-type contributions from four configuration series have been evaluated and presented in columns 2 to 5 in Table 3. The calculated results indicate that the absolute values from the pp and pf series are comparable but with opposite signs, while those from the sd and dd series are trivial. As to the CC-type, only the pp series are concerned and the results are listed in column 6. It is obvious that the CC-type contributions are small enough to be neglected. The net sums of the BC-type contributions are presented in the last column of Table 3 and are much smaller than those of the corresponding BB-type because of the counteractions between pp and pf series. We take the total results of the second-order perturbation corrections as reference to the selection of configuration series in the third-order perturbation calculation.

Table 4 gives the third-order contributions to exchange terms. As to the similarity between the later terms of (6) and the second-order perturbation formula, the contributions of this term could be treated in a similar way as in the second-order perturbation, as to the residue processing. These results are listed in the fourth and fifth columns, where the former contain the contribution from BB-type only and the latter are those of the BC-type. Such a huge difference of nine orders could be observed. The former

Table 4. Calculated results of the third-order perturbation corrections (GHz). According to (6), contributions from the former and latter terms are calculated, respectively.

n	Sum. of bounds for the 1st term	Int. of continua for the 1st term	Sum. of bounds for the 2nd term	Int. of bounds for the 2nd term	Total
12	0.521	2.655(-5)	1.093(-2)	-5.067(-12)	0.532
13	0.410	2.098(-5)	7.353(-3)	-3.159(-12)	0.417
14	0.328	1.686(-5)	5.090(-3)	-2.037(-12)	0.333
15	0.267	1.374(-5)	3.613(-3)	-1.353(-12)	0.271
16	0.220	1.135(-5)	2.621(-3)	-9.224(-13)	0.223
17	0.183	9.482(-6)	1.938(-3)	-6.432(-13)	0.185
18	0.154	8.001(-6)	1.458(-3)	-4.577(-13)	0.155
19	0.131	6.812(-6)	1.113(-3)	-3.317(-13)	0.132
20	0.112	5.848(-6)	8.621(-4)	-2.443(-13)	0.113

Table 5. $^1D-^3D$ term intervals and comparisons to theoretical and experimental data (GHz).

n	First-order	Second-order	Third-order	Total	Expt. [30]	Expt. [31]
12	4.866	-2.550	0.532	2.848	2.872	2.862
13	3.844	-2.014	0.417	2.247	2.269	2.258
14	3.089	-1.618	0.333	1.804	1.823	1.812
15	2.519	-1.319	0.271	1.471	1.486	1.475
16	2.080	-1.091	0.223	1.212	1.227	1.215
17	1.738	-0.912	0.185	1.011	1.025	1.013
18	1.466	-0.769	0.155	0.852	0.865	0.852
19	1.249	-0.655	0.132	0.726	0.737	0.707
20	1.072	-0.562	0.113	0.623	0.632	0.596

term of (6) includes quadruple summations (or integrals). It is very complicated to evaluate over various configuration series. For simplicity, only the pp and sd configuration series have been included in the evaluation of BB-type contributions, while the pp and pf series are employed in the BC-type. The calculated results are shown in columns 2 and 3, respectively. Comparison of the results reveals that the dominant contributions mainly come from the summations over bound states. And the contributions from the former term in (6) are more important than those of the latter one.

Table 5 presents the final results of helium $^1D-^3D$ term intervals for $1snd$ ($n = 12 \sim 20$) Rydberg states and the comparisons with the experiments. Columns 2–4 give the exchange energies of the first-, second-, and third-order perturbation corrections. Summations of these values give the net result, which is in the fifth column. And the last two columns are the experimental results [30, 31]. Singlet–triplet level splittings yielded here have been found to be in accord with these results.

From Table 5, it can also be foreseen that contributions of the fourth-order perturbation will be negative, which will make the final results lower than the present ones. But the effects of magnetic or spin-dependent interactions with their nondiagonal matrix elements [29], which are not included in this work either, will counteract the contributions of the fourth-order perturbation in a certain scale. Such investigations are worthy of further research.

4. Conclusion

How to choose zeroth-order solutions in a perturbation calculation is critical. Based on two different models, the perturbation expansion terms consisting of bound states only and those of continua have

been evaluated, respectively. As to the former, zeroth-order wave functions have been constructed from the solutions of the Hartree equation based on the first principle and the residues of the summation series are dealt with using the integral processing method, while a simplified hydrogen potential has been applied to obtain the continuum wave functions. A large integral range is used to lead the residues of the integral over continua to be negligible. The calculated results indicate that the summation series over bound states dominates the second- and third- order perturbation corrections to the level splittings.

We have utilized an improved Numerov algorithm [27, 28] to ensure the numerical efficiency and the quantitative accuracy for higher Rydberg states and the continua and computed with double precision to ensure the float calculation. Singlet–triplet level splitting for helium $1snd$ ($n = 12 \sim 20$) configurations yielded here are found to agree quite well with two sets of experimental results, especially for higher Rydberg configurations.

Acknowledgements

This work was supported by the National Natural Science Foundation of China No. 10575037, the foundation of East China University of Science and Technology and Swiss National Science Foundation. We want to stress our sincere thanks to Professors J.-Z. Zhang and J.-Cl. Dousse. Our appreciation is also given to Professor Y.-H. Luo.

References

1. N.H. Linder, A. Peres, and D.R. Terno. Phys. Rev. A, **68**, 042308 (2003).
2. N.N. Nedeljković, Lj.D. Nedeljković, and M.A. Mirković. Phys. Rev. A, **68**, 012721 (2003).
3. J.-Z. Zhang. Phys. Rev. Lett. **93**, 043002 (2004).
4. T. Gallagher. Rydberg atoms. Cambridge University Press, Cambridge. 1994.
5. I. Lindgren and J. Morrison. Atomic many-body theory. Springer-Verlag, Berlin, New York. 1986.
6. T.-N. Chang. Many-body theory of atomic structure and photoionization. World Scientific, Singapore. 1993.
7. J.J. Boyle and M.S. Pindzola. Many-body atomic physics: lecture on the application of many-body theory to atomic physics. Cambridge University Press, Cambridge. 1998.
8. H.P. Kelly. Phys. Rev. B, **136**, 3896 (1964).
9. T.-N. Chang and R.T. Poe. Phys. Rev. A, **10**, 1981 (1974).
10. T.-N. Chang and R.T. Poe. Phys. Rev. A, **14**, 11 (1976).
11. T.-N. Chang. Phys. Rev. A, **39**, 4946 (1989).
12. W.R. Johnson, S.A. Blundell, and J. Sapirstein. Phys. Rev. A, **37**, 307 (1988).
13. J.S. Sims and W.C. Martin. Phys. Rev. A, **37**, 2259 (1988).
14. G.W.F. Drake. Phys. Rev. Lett. **59**, 1549 (1987).
15. G.W.F. Drake. Phys. Rev. Lett. **65**, 2769 (1990).
16. G.W.F. Drake. J. Phys. B: At. Mol. Opt. Phys. **22**, L651 (1989).
17. A. Wasserman, N.T. Maitra, and K. Burke. Phys. Rev. Lett. **91**, 263001 (2003).
18. A.K. Roy and S.-I. Chu. Phys. Rev. A, **65**, 052508 (2002).
19. Z. Zhou and S.-I. Chu. Phys. Rev. A, **71**, 022513 (2005).
20. I.M. Savukov and W.R. Johnson. Phys. Rev. A, **65**, 042503 (2002).
21. V.A. Dzuba, V.V. Flambaum, and M.G. Kozlov. Phys. Rev. A, **54**, 3948 (1996).
22. V.A. Dzuba and W.R. Johnson. Phys. Rev. A, **57**, 2459 (1998).
23. E.P. Vidolova-Angelova, L.N. Ivanov, and V.S. Letodhov. J. Opt. Soc. Am. **71**, 6699 (1981).
24. K. Koc and J. Migdalec. J. Phys. B: At. Mol. Opt. Phys. **23**, L5 (1990).
25. C. Froese Fischer. Computational atomic structure: an MCHF approach. Bristol Institute of Physics Publication. 1997.
26. R.D. Cowan. The theory of atomic structure and spectra. University of California Press, Berkeley, Los Angeles, London. 1981.
27. L.-M. He, H. Lu, and Y. Yang. Chin. J. At. Mol. Phys. **19**, 316 (2002).
28. L.-M. He, Y. Yang, and H. Lu. Act. Phys. Sin. **52**, 1385 (2003).

29. E.A. Hessels, W.G. Sturuss, and S.R. Lundeen. *Phys. Rev. A*, **35**, 4489 (1987).
30. J.W. Farley, K.B. MacAdam, and W.H. Wing. *Phys. Rev. A*, **20**, 1754 (1979).
31. H.J. Beyer and K.J. Kollath. *J. Phys. B: At. Mol. Opt. Phys.* **9**, L185 (1976).